Origin of gap anisotropy in spin fluctuation models of the iron pnictides

T. A. Maier[*]

*Center for Nanophase Materials Sciences and Computer Science and Mathematics Division, Oak Ridge National Laboratory,
Oak Ridge, Tennessee 37831-6494, USA*

S. Graser[†]

Center for Electronic Correlations and Magnetism, Institute of Physics, University of Augsburg, D-86135 Augsburg, Germany

D. J. Scalapino[‡]

Department of Physics, University of California, Santa Barbara, California 93106-9530, USA

P. J. Hirschfeld[§]

Department of Physics, University of Florida, Gainesville, Florida 32611, USA

We discuss the large gap anisotropy found for the A_{1g} (s wave) state in random-phase approximation spin fluctuation and functional renormalization-group calculations and show how the simple arguments leading to isotropic sign-switched s-wave states in these systems need to be supplemented by a consideration of pair scattering within Fermi-surface sheets and between the individual electron sheets as well. In addition, accounting for the orbital makeup of the states on the Fermi surface is found to be crucial.

PACS number(s): 74.20.Mn, 74.20.Rp

With one or two exceptions, the newly discovered Fe-pnictide superconductors are created by doping parent materials which manifest a magnetically ordered ground state. Since critical temperatures are as high as 56 K and experiments have shown enhanced magnetic response relative to *ab initio* electronic structure calculations, it is natural to consider spin fluctuation-type pairing models for these systems. There have been several calculations of this general type, which have reported gaps with significant anisotropy on the multisheeted Fermi surface of these materials.[1–10] For the most part, a ground state with A_{1g} symmetry has been identified, with a nearby $d_{x^2-y^2}$ (in the unfolded Brillouin zone) pairing eigenvalue. These calculations involve fairly realistic representations of the electronic structure near the Fermi surface and are sufficiently complicated that the precise physical effects leading, e.g., to a particular pairing channel or to gap anisotropy, can be obscured.

At the same time, there is a simple argument originally given by Mazin *et al.*,[11] which suggests that the order parameter in the system should have a sign-switched s-wave structure.[8,10–13] It is based on the argument that the scattering of pairs between the α-hole Fermi surfaces around the Γ point and the β-electron Fermi surfaces around the $X(\pi,0)$ and $Y(0,\pi)$ points of the unfolded Brillouin zone (see Fig. 1) is dominant in the system due to the near nesting of the small sheets. In this picture, the system can maximize its condensation energy by forming isotropic order parameters but switching sign between the α and β sheets to take advantage of the interband pair scattering. This change in sign has the added benefit of reducing the short-range on-site Coulomb repulsion.[14] It is therefore, at first sight, surprising to find that random-phase approximation (RPA) spin fluctuation calculations[1,15] as well as functional renormalization-group studies[9] find a highly anisotropic A_{1g} s-wave gap. Here, we investigate this, as well as explore the question of what the

anisotropy can tell us about the pairing interaction. One answer that has been given is that the momentum dependence of the fluctuation-exchange pairing interaction can drive the anisotropy.[2,15] However, we will see that the orbital makeup of the states on the Fermi surface and the suppression of the short-range Coulomb interaction[13] also play key roles in favoring an anisotropic gap. The gap anisotropy was also discussed in two recent studies. The role of the intra-Fermi-surface Coulomb scattering has been discussed in Ref. 16 and the variation in the inter-Fermi-surface spin fluctuation interaction with the height of the pnictogen ion has been studied in Ref. 17. In the following, we examine the pairing strengths for processes which involve a pair of electrons scattering on and between the four Fermi surfaces shown in Fig. 1.
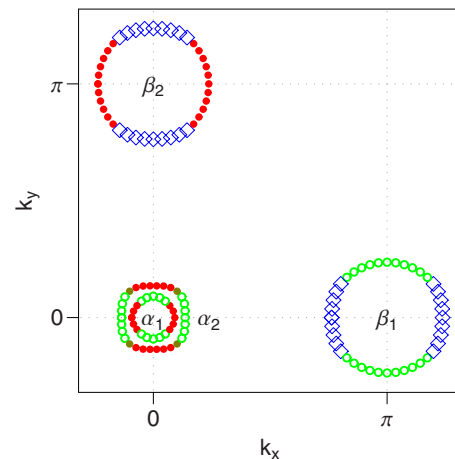

FIG. 1. (Color online) The Fermi surface of the five-orbital tight-binding model (Ref. 15). The main orbital contributions are shown by the following colors/symbols: d_{xz} (red/solid circles), d_{yz} (green/open circles), and d_{xy} (blue/diamonds).
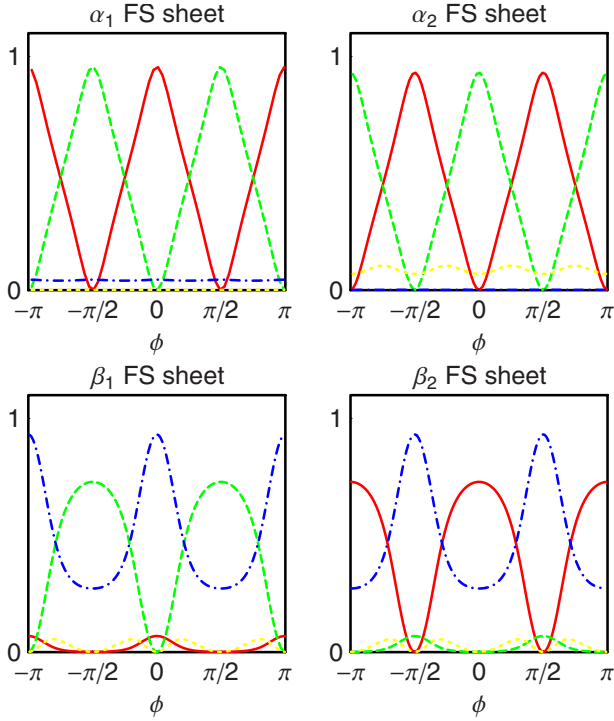
FIG. 2. (Color online) The orbital weights as a function of the winding angle ϕ on the different Fermi-surface sheets (Ref. 15). The different colors/lines refer to d_{xz} (red/solid lines), d_{yz} (green/dashed lines), d_{xy} (blue/dash-dotted line), and $d_{x^2-y^2}$ (yellow/short-dashed line).

These were calculated using a five-orbital $(d_{xz}, d_{yz}, d_{xy}, d_{x^2-y^2}, d_{3z^2-r^2})$ tight-binding fit to the density-functional theory band-structure calculations of Cao *et al.*[18] The tight-binding parameters for an orbital basis that is aligned parallel to the nearest-neighbor Fe-Fe direction are given in the Appendix of Ref. 15. Here we will label the two hole Fermi surfaces α_1 and α_2 and the two electron Fermi surfaces β_1 and β_2 as indicated in Fig. 1.

The orbital weights $a_i^t(k)$ of the states on the various Fermi surfaces are shown in Fig. 2 and illustrated by the colors in Fig. 1. Here i designates the Fermi sheet α_1, α_2, β_1, and β_2 and t is the orbital $(d_{xz}, d_{yz}, \ldots)$. The dominant orbitals contributing to the α_1 and α_2 sheets are the d_{xz} and d_{yz} orbitals. The upper and lower parts of the α_1 sheet are d_{yz} like and the left- and right-hand sides have d_{xz} character. The opposite behavior is seen on the α_2 sheet. On the β_1 sheet, the upper and lower surfaces have dominantly d_{yz} character, while the ends along the k_x axis have d_{xy} character. Similarly, the β_2 sheet is made up of d_{xz} along the sides and d_{xy} on the k_y axis ends.[11,15,19]

Now consider the scattering of a pair $(k'\uparrow, -k'\downarrow)$ on the α_1 Fermi surface to a pair $(k\uparrow, -k\downarrow)$ on the β_1 Fermi surface. The strength of this scattering depends upon

$$\Gamma_{ij}(k,k') = \sum_{stpq} a_{\nu_i}^{t,*}(-k) a_{\nu_i}^{s,*}(k) \mathrm{Re}[\Gamma_{st}^{pq}(k,k',0)] a_{\nu_j}^{p}(k') a_{nu_j}^{q}(-k')$$

(1)

and involves orbital weight factors and, within the fluctuation-exchange approximation, the orbital-dependent vertex

$$\Gamma_{st}^{pq}(k,k') = \left[\frac{3}{2}\left(U^s \chi_s^{\mathrm{RPA}} U^s + \frac{U^s}{2} \right) - \frac{1}{2}\left(U^c \chi_c^{\mathrm{RPA}} U^c - \frac{U^c}{2} \right) \right]_{ps}^{tq}.$$

(2)

Here, the momenta k and k' are restricted to the different Fermi-surface sheets C_i with $k \in C_i$ and $k' \in C_j$. The interaction matrices U^s and U^c contain the on-site intra- and inter-Coulomb interactions along with the exchange couplings and χ_s^{RPA} and χ_c^{RPA} are the RPA spin- and charge-orbital susceptibilities. We will use numerical results obtained from earlier work,[20] but our results are not dependent on the precise values of the parameters. Rather, what is important to note is that the dominant pairing interaction is found to arise from the spin fluctuation term $\frac{3}{2} U^s \chi_s^{\mathrm{RPA}} U^s$, while the short-range Coulomb contact interactions $\frac{3}{4} U^s$ and $\frac{U^c}{4}$ oppose the pairing. As noted by Mazin and Schmalian,[14] for a simple two-band model with equal density of states, the short-range Coulomb repulsion vanishes for a sign-switched *s*-wave gap. However, as they point out, when there is an asymmetry in the density of states, some fraction of the Coulomb repulsion remains. We will see that it is both the orbital weight factors and the further suppression of the Coulomb interaction that lead to the anisotropy of the gap in the realistic case.

First, we discuss the effect of the orbital matrix elements. The scattering strength $\Gamma_{ij}(k_0,k)$ for two different pairs on the α_1 sheet with $\mathbf{k}_0 = (k_F, 0)$ and $\mathbf{k}_0 = (0, k_F)$ as a function of momentum k are illustrated in Fig. 3. For the former [Fig. 3(a)], the dominant scattering is to $d_{xz}(k\uparrow, -k\downarrow)$ pairs on the β_2 Fermi surface and for the latter [Fig. 3(b)] to d_{yz} pairs on the β_1 Fermi surface. Note that the scattering strength is not simply a consequence of nesting; instead, it reflects the orbital weight structure factors. The $d_{xz}(k'\uparrow, -k'\downarrow)$ pairs on α_1 scatter more strongly to $d_{xz}(k\uparrow, -k\downarrow)$ pair states on β_2 than to pair states on the β_1 Fermi surface which involve other orbitals. This means that while it is in general favorable to have a sign change between the gaps on the α_1 and β_2 Fermi surfaces, the essential thing is to have a sign change in the gap between the red (d_{xz}) regions of the α_1 Fermi surface and the red (d_{xz}) parts of the β_2 Fermi surface shown in Fig. 1. Likewise, one needs a sign change between the green (d_{yz}) regions of the α_1 Fermi surfaces and the green (d_{yz})β_1 Fermi surface. It is not important to maintain this sign change in the yellow (d_{xy}) regions of the β Fermi surfaces. We will in fact see that the magnitude of the gap is larger on the d_{yz} portion of the β_1 Fermi surface and smaller on the d_{xy} parts. This actually leads to a small increase in the α-β_1 pairing compared to the isotropic sign-switched gap.

In addition, as we will discuss, if there are other interactions such as the local Coulomb interaction or scattering processes, such as inter-Fermi-surface β_1-β_2 scattering, reducing the magnitude or even changing the sign of the gap on the d_{xy} part of the β Fermi surfaces can lead to an additional reduction in the short-range Coulomb interaction and an enhancement of the pairing. In order to explore this latter effect, we need to obtain a more detailed accounting of the
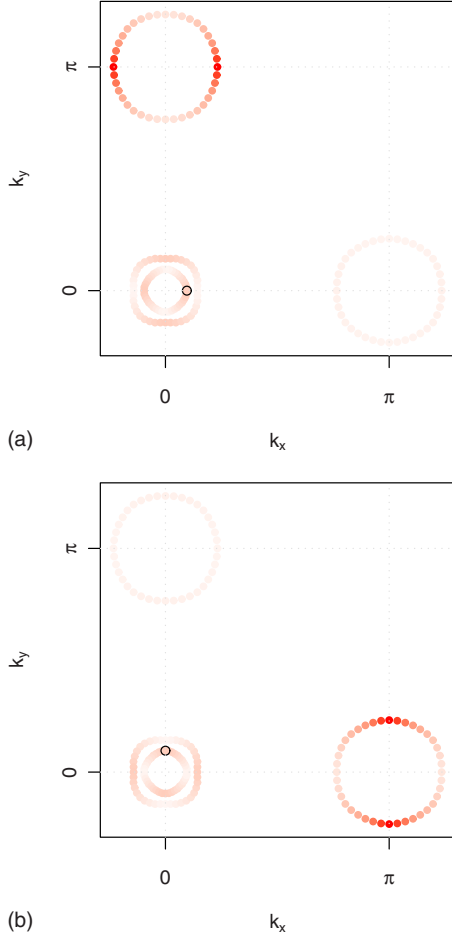
(a)

(b)

FIG. 3. (Color online) The strength $\Gamma_{ij}(k_0,k)$ associated with scattering a pair from the α_1 Fermi surface with momenta (a) $k_0 = (k_F\hat{\imath}, -k_F\hat{\imath})$ and (b) $k_0 = (k_F\hat{\jmath}, -k_F\hat{\jmath})$ as indicated by the black circles as a function of momentum k. The orbital weight factors favor scattering from d_{xz} to d_{xz} and d_{yz} to d_{yz} orbital states.

various contributions to the pairing strength. As discussed in Ref. 15, for a given gap function $g(k)$, the effective pairing strength is determined from

$$\lambda[g(k)] = -\frac{\Sigma_{ij}\oint_{C_i}\dfrac{dk_\parallel}{v_F(k)}\oint_{C_j}\dfrac{dk'_\parallel}{v_F(k')}g(k)\Gamma_{ij}(k,k')g(k')}{(2\pi)^2\Sigma_i\oint_{C_i}\dfrac{dk_\parallel}{v_F(k)}[g(k)]^2}.$$

$$(3)$$

Here $v_F(k) = |\nabla_k E_i(k)|$ for k on a given Fermi surface C_i. In the following, we will normalize the gap function $g(k)$ such that the denominator is equal to the total one-electron density of states,

$$\sum_j\oint_{C_j}\frac{dk_\parallel g^2(k)}{2\pi[2\pi v_F(k)]} = \sum_j N_j(0). \qquad (4)$$

Then we can decompose λ into its contributions from the different inter- and intra-Fermi-surface scattering processes,

$$\lambda[g] = \sum_{ij}\lambda_{ij}[g], \qquad (5)$$

with

$$\lambda_{ij}[g] = -\oint_{c_i}\frac{dk_\parallel}{2\pi[2\pi v_F(k)]}\oint_{c_j}\frac{dk'_\parallel}{2\pi[2\pi v_F(k')]}$$

$$\times\frac{g(k)\Gamma_{ij}(k,k')g(k')}{\sum_i N_i(0)}. \qquad (6)$$

First, consider λ_{ij} for two limiting cases: (1) the optimal RPA $g(k)$ found as the variational solution of Eq. (3) and (2) a sign-switched s wave with $g_{\alpha_1} = g_{\alpha_2} = 1$ and $g_{\beta_1} = g_{\beta_2} = -1$. The results are shown in Figs. 4 and 5. The total pairing strength is significantly larger for the highly anisotropic RPA $g(k)$. From the breakdown of the various contributions, one sees that while the total α-β contribution is larger (0.23 compared with 0.21), for the sign-switched gap function, the larger negative contribution of the Fermi surface λ's as well as the larger negative β_1-β_2 contribution overcome this and λ for the sign-switched gap is considerably smaller than the optimal λ. In Fig. 4, one can see that the anisotropy of the RPA solution is such that there are nodes on the β sheets.[21] These results for the anisotropy of the gap are based upon an exchange fluctuation approach and are applicable to the weak to intermediate coupling regime. As we will discuss, whether this happens or not depends upon the parameters. The interplay of the orbital weights in the pairing interaction (3) and the reduction in the intra-β_1-β_1 Coulomb interaction, as well as the inter-β_1-β_2 scattering lead to the anisotropy.

To illustrate this, consider the simple parametrization of an anisotropic gap with $g_{\alpha_1} = g_{\alpha_2} = 1$ and

$$g_\beta = -a(1 - r\cos 2\theta). \qquad (7)$$

Here $a = [2/(2+r^2)]^{1/2}$ so that the normalization condition (4) is satisfied. When $r = 0$, $g_\beta = -1$ and we have the sign-switched state previously discussed. Then as r increases, the gap function becomes anisotropic on the β Fermi surfaces as shown in Fig. 6. In Fig. 7 we plot the total pairing strength λ and some of its components versus r. Initially, as r increases, the gap on the β Fermi-surface sheets becomes anisotropic, and the total pairing strength λ increases. The slight increase in $\lambda_{\alpha\text{-}\beta}$ reflects the increase in the amplitude of the gap in the regions where the d_{xz} and d_{yz} orbital weights are largest. The additional increase in λ arises from the suppression of the intra- and inter-Coulomb repulsions associated with the β_1 and β_2 Fermi surfaces due to the gap anisotropy. Finally, as r increases further, the reduction in the α-β pairing contribution due to the anisotropy becomes larger than the suppression of the Coulomb interaction and the total pairing strength λ decreases. For the interaction parameter set that we are using, this occurs for $r \simeq 1.5$, so that there are well-developed nodes on the β-Fermi surfaces. However, if the pair scattering within and between the β sheets were reduced, the nodes could be lifted.

The anisotropy of the A_{1g} gap on the electron Fermi surfaces found in RPA and numerical functional renormalization-group studies has been shown to arise from
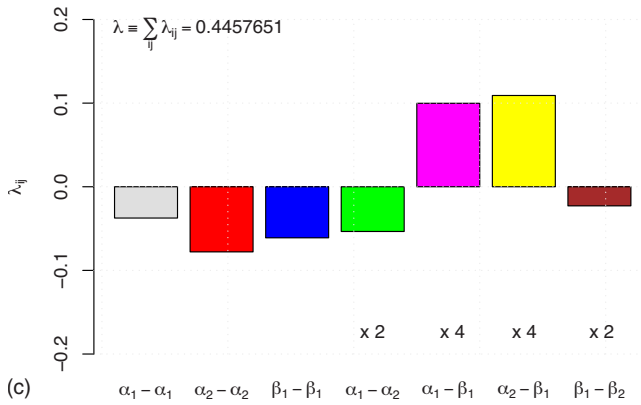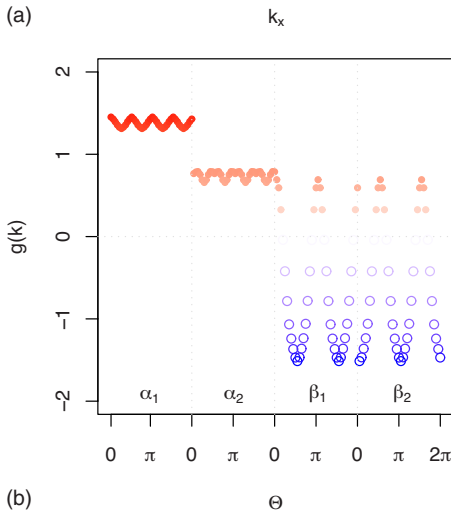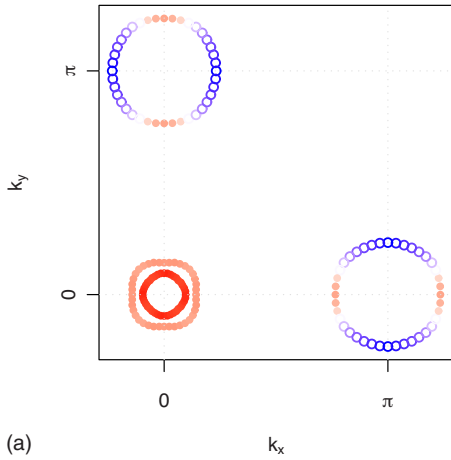
FIG. 4. (Color online) The RPA gap function (a) plotted on the Fermi surfaces (red/solid circles positive and blue/open circles negative), (b) $g(k)$ as a function of angle, and (c) bar graph of the various interaction components λ_{ij}. Note that the off-diagonal terms contribute to the total λ [Eq. (5)] with weights of two or four as indicated.

FIG. 5. (Color online) The sign-switched gap function (similar to Fig. 4).

an interplay of three sources: (1) the variation in the weighting of the different d orbitals on the Fermi surfaces, (2) the need to suppress the Coulomb repulsion, and (3) the need to reduce the effects of the repulsive scattering between the electron-β sheets. The orbital weight variation is familiar in other multiorbital superconductors such as MgB$_2$.[22] In essence, the pairing interaction is strongest between fermions
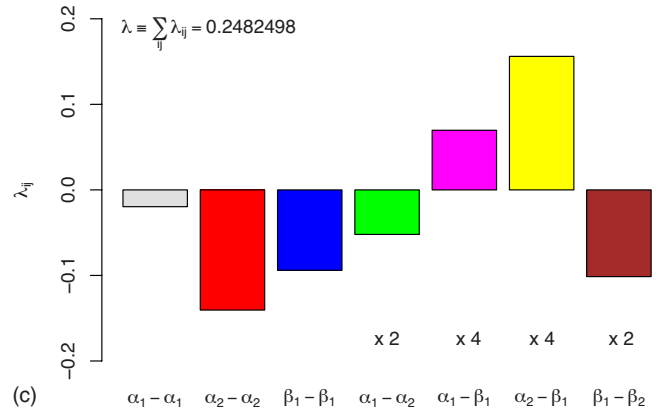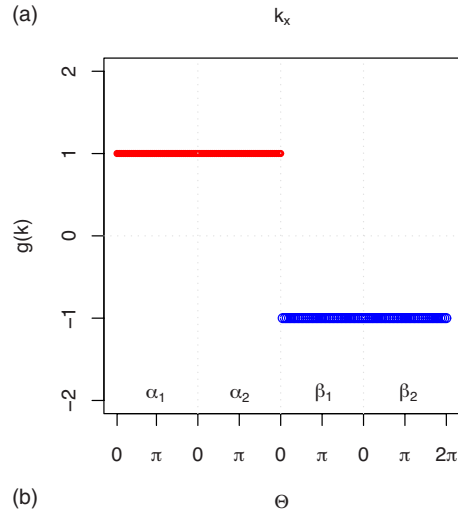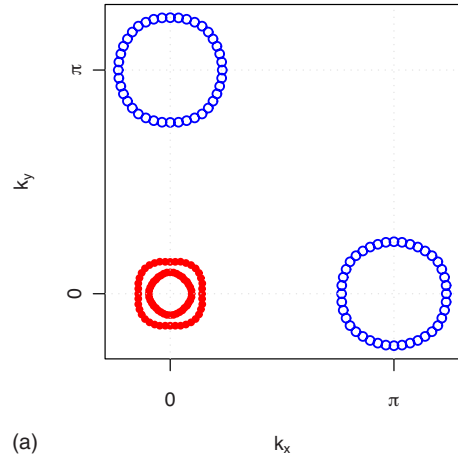
in near-neighbor d_{yz} orbitals along the x direction and near-neighbor d_{xz} orbitals along the y direction. The pairing associated with the d_{xy} near-neighbor orbitals is weaker. At the same time, the anisotropy leads to a reduction in the repulsive Coulomb interactions and the inter-Fermi-surface β_1-β_2 scattering. As discussed, there is a balance between these effects which determine whether the anisotropy is sufficiently large that there are nodes on the β sheets. The fact that the dominant orbital weights on the α_1 and α_2 Fermi surfaces are associated with the d_{xz} and d_{yz} orbitals leads to a more isotropic gap on these sheets.
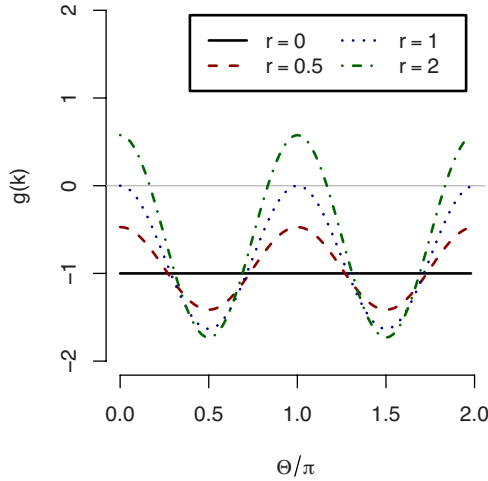
FIG. 6. (Color online) The phenomenological anisotropic gap function on the β-Fermi surface versus angle for several different values of r.

The results that we have discussed are based upon a weak-coupling spin fluctuation approach. In particular, the various calculations have used an RPA form for the pairing vertex. Here the band structure and filling, along with the relative strengths of the on-site Coulomb and exchange interactions enter. A key feature of this approach is that the gap exhibits large anisotropies and that nodes may appear on the β-Fermi surfaces in the s-wave A_{1g} state. However, one can imagine that variations in the parameters can alter the degree of anisotropy. An important implication of this is that it may provide an explanation for the wide variety of experimental indications that nodes are present in some cases and not in others. Another explanation for these apparent discrepancies could be the degree of disorder in different samples as discussed in Refs. 10 and 23–25.
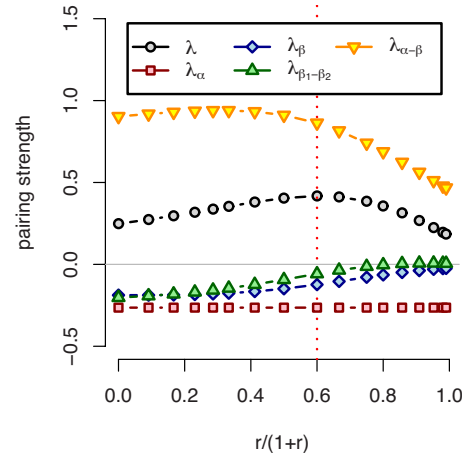

FIG. 7. (Color online) The pairing strength and its components versus r for the anisotropic gap shown in Fig. 6. Here, λ is the total pairing strength. The intra- and inter-α_1 and α_2 Fermi-surface contributions are given by $\lambda_\alpha = \lambda_{\alpha_1 \alpha_1} + \lambda_{\alpha_2 \alpha_2} + 2\lambda_{\alpha_1 \alpha_2}$ and the intra-β Fermi-surface contribution by $\lambda_\beta = \lambda_{\beta_1 \beta_1} + \lambda_{\beta_2 \beta_2}$. The contribution to the pairing comes from $\lambda_{\alpha-\beta} = 4\lambda_{\alpha_1 \beta_1} + 2\lambda_{\alpha_2 \beta_1}$, while for this A_{1g} gap, the inter-β_1-β_2 contribution opposes the pairing for small r and is neutralized for a large anisotropy. The red dashed line indicates the optimal degree of anisotropy $r = 1.5$.

*maierta@ornl.gov

†graser@phys.ufl.edu

‡djs@physics.ucsb.edu

§pjh@phys.ufl.edu

[1] K. Kuroki, S. Onari, R. Arita, H. Usui, Y. Tanaka, H. Kontani, and H. Aoki, Phys. Rev. Lett. **101**, 087004 (2008).

[2] K. Kuroki, S. Onari, R. Arita, H. Usui, Y. Tanaka, H. Kontani, and H. Aoki, Phys. Rev. Lett. **102**, 109902(E) (2009).

[3] K. Kuroki, S. Onari, R. Arita, H. Usui, Y. Tanaka, H. Kontani, and H. Aoki, New J. Phys. **11**, 025017 (2009).

[4] X. Qi, S. Raghu, C. Liu, D. Scalapino, and S. Zhang, arXiv:0804.4332 (unpublished).

[5] V. Barzykin and L. Gorkov, JETP Lett. **88**, 131 (2008).

[6] Y. Bang and H. Y. Choi, Phys. Rev. B **78**, 134523 (2008).

[7] Z. Yao, J. Li, and Z. Wang, New J. Phys. **11**, 025009 (2009).

[8] R. Sknepnek, G. Samolyuk, Y. B. Lee, and J. Schmalian, Phys. Rev. B **79**, 054511 (2009).

[9] F. Wang, H. Zhai, Y. Ran, A. Vishwanath, and D. H. Lee, Phys. Rev. Lett. **102**, 047005 (2009).

[10] A. V. Chubukov, D. V. Efremov, and I. Eremin, Phys. Rev. B **78**,

134512 (2008).

[11] I. I. Mazin, D. J. Singh, M. D. Johannes, and M. H. Du, Phys. Rev. Lett. **101**, 057003 (2008).

[12] Y. Yanagi, Y. Yamakawa, and Y. Ono, J. Phys. Soc. Jpn. **77**, 123701 (2008).

[13] A. Chubukov, arXiv:0902.4188 (unpublished).

[14] I. Mazin and J. Schmalian, arXiv:0901.4790 (unpublished).

[15] S. Graser, T. A. Maier, P. J. Hirschfeld, and D. J. Scalapino, New J. Phys. **11**, 025016 (2009).

[16] A. Chubukov, M. Vavilov, and A. Vorontsov, arXiv:0903.5547 (unpublished).

[17] K. Kuroki, H. Usui, S. Onari, R. Arita, and H. Aoki, arXiv:0904.2612 (unpublished).

[18] C. Cao, P. J. Hirschfeld, and H. P. Cheng, Phys. Rev. B **77**, 220506(R) (2008).

[19] P. A. Lee and X. G. Wen, Phys. Rev. B **78**, 144517 (2008).

[20] Here we have set the on-site intraorbital $U = 5/3$, the exchange $J = 2J' = U/8$, and the interorbital $V = U - 3/4J - J'$. These represent typical parameters for which the leading pairing strength

occurs in the singlet A_{1g} state. We find similar behavior for a range of parameters.

[21] We have also examined a parameter range in which a $d_{x^2-y^2}B_{1g}$ gap is favored. Here, the anisotropy occurs on the α_1 and α_2 Fermi surfaces where the gap has $d_{x^2-y^2}$ symmetry. This is dominantly driven by the α-β scattering processes and arises naturally from the sign change in the gap on the β_1 Fermi surface relative to the gap on the β_2 Fermi surface for the B_{1g} state.

[22] H. J. Choi, D. Roundy, H. Sun, M. L. Cohen, and S. G. Louie, Nature (London) **418**, 758 (2002).

[23] V. Mishra, G. Boyd, S. Graser, T. Maier, P. J. Hirschfeld, and D. J. Scalapino, Phys. Rev. B **79**, 094512 (2009).

[24] A. Vorontsov, M. Vavilov, and A. Chubukov, Phys. Rev. B **79**, 140507(R) (2009).

[25] D. Parker, O. V. Dolgov, M. M. Korshunov, A. A. Golubov, and I. I. Mazin, Phys. Rev. B **78**, 134524 (2008).